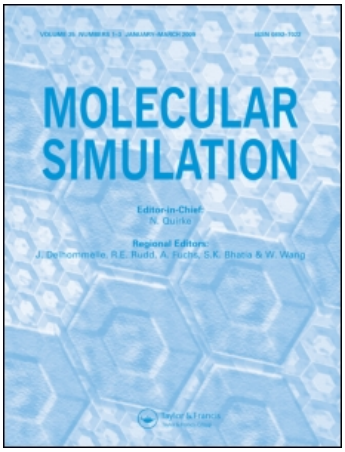

Molecular Simulation
Publication details, including instructions for authors and subscription information:
http://www.informaworld.com/smpp/title~content=t713644482

Ab initio fragment molecular orbital calculations on the specific interactions between human, mouse and rat PPARα and GW409544

Masato Hayakawa[a]; Tatsuya Ohyama[a]; Yoko Yamaguchi[a]; Shingo Iwabuchi[a]; Tomohiko Nakagawa[b]; Tamie Nakajima[b]; Noriyuki Kurita[a]
[a] Department of Knowledge-based Information Engineering, Toyohashi University of Technology, Toyohashi, Aichi, Japan [b] Department of Occupational Environmental Health, Graduate School of Medicine, Nagoya University, Nagoya, Japan

Online publication date: 16 August 2010

To cite this Article Hayakawa, Masato , Ohyama, Tatsuya , Yamaguchi, Yoko , Iwabuchi, Shingo , Nakagawa, Tomohiko , Nakajima, Tamie and Kurita, Noriyuki(2010) '*Ab initio* fragment molecular orbital calculations on the specific interactions between human, mouse and rat PPARα and GW409544', Molecular Simulation, 36: 9, 644 — 656
To link to this Article: DOI: 10.1080/08927021003671566
URL: http://dx.doi.org/10.1080/08927021003671566

Molecular Simulation
Vol. 36, No. 9, August 2010, 644–656

Taylor & Francis
Taylor & Francis Group

Ab initio fragment molecular orbital calculations on the specific interactions between human, mouse and rat PPARα and GW409544

Masato Hayakawa[a], Tatsuya Ohyama[a], Yoko Yamaguchi[a], Shingo Iwabuchi[a], Tomohiko Nakagawa[b], Tamie Nakajima[b] and Noriyuki Kurita[a]*

[a]*Department of Knowledge-based Information Engineering, Toyohashi University of Technology, Tempaku-cho, Toyohashi, Aichi 441-8580, Japan;* [b]*Department of Occupational Environmental Health, Graduate School of Medicine, Nagoya University, 65 Tsurumaicho, Showa-ku, Nagoya 446-8550, Japan*

(*Received 2 March 2009; final version received 2 February 2010*)

To elucidate the specific interactions between the peroxisome proliferator-activated receptor (PPARα) and ligand GW409544 (GW), we obtained the solvated structures of the PPARα+GW complexes for human, mouse and rat by classical molecular mechanics calculations, and investigated their electronic properties by *ab initio* fragment molecular orbital calculations. The results indicate that the positively charged amino acids (Lys and Arg) of PPARα make a major contribution to the binding between PPARα and GW. In addition, it was clarified that Ser280 and Tyr314 of human and rat PPARα have a large attractive interaction with GW, while Ser280, Tyr314 and His440 of mouse PPARα have large interaction. These results on the difference in specific interactions between human and mouse/rat PPARα will be useful for predicting the effects of new chemicals on the human body based on the biomedical studies for the experimental animals such as mouse and rat.

Keywords: peroxisome proliferator-activated receptor; specific interactions; electronic properties; *ab initio* molecular orbital calculation; molecular mechanics

1. Introduction

Nuclear receptors exist in the cell nucleus and control the appearance of important genes for maintaining the vital functions such as glucidic and lipid metabolising, bone metabolising, anti-inflammation action and immunity control. Peroxisome proliferator-activated receptor (PPAR) belongs to the superfamily of nuclear receptors and controls the production of various proteins related to the metabolism of lipid and glucidic at the gene level [1]. Additionally, the heterodimer of PPAR and the retinoid X receptor having 9-*cis* retinoic acid as an endogenous agonist affects the peroxisome proliferator response element to promote the transcription reaction. Under the condition without the agonist, the co-repressor binds to the heterodimer to repress the transcription reaction. On the other hand, by the binding of the agonist, the heterodimer releases the co-repressor and bonds the co-activator, resulting in the activation of the gene expression.

PPAR has three subtypes, α, γ and δ. All subtypes have DNA binding domain on the N-terminal side and ligand binding domain (LBD) on the C-terminal side. Recent biomedical studies have shown that PPAR takes part in many kinds of diseases such as diabetes [2], cancer [3] and inflammatory disorder [4]. In addition, PPAR is considered to have a strong relationship with the development of toxicity induced by environmental pollutants [5]. However, the function of PPAR in the mechanism of toxicity development and the specific bonding mechanism of PPAR and ligand molecules are not yet clarified at the atomic level.

In the present study, we investigate the specific interactions between human, mouse and rat PPARα and ligand GW409544 (GW), whose chemical structure is shown in Figure 1(a). PPARα controls the expression of genes contributing to the fatty acid metabolism and makes an adjustment of lipid metabolism. The experimental study [6] reported that the expression is enhanced about 500 times by the administration of GW, in comparison with the administration of the AZ242 ligand (Figure 1(b)). We thus employed GW as the ligand to PPARα. Human, mouse and rat PPARα are composed of 468 amino acid residues. As shown in Figure 2, there are 21 differences in amino acids of LBD between human and mouse PPARα, while there are 19 differences between human and rat PPARα [7]. The 3D structure of human PPARα was obtained by the X-ray crystal structure analysis [8]. On the other hand, the structures of mouse and rat PPARα are not yet clarified. In order to explain the difference in the functions of human, mouse and rat PPARα, it is indispensable to elucidate the 3D structures of these PPARα with and without the ligand molecule. In particular, it is essential to elucidate the difference in specific interactions between

*Corresponding author. Email: kurita@tutkie.tut.ac.jp

ISSN 0892-7022 print/ISSN 1029-0435 online

DOI: 10.1080/08927021003671566
http://www.informaworld.com

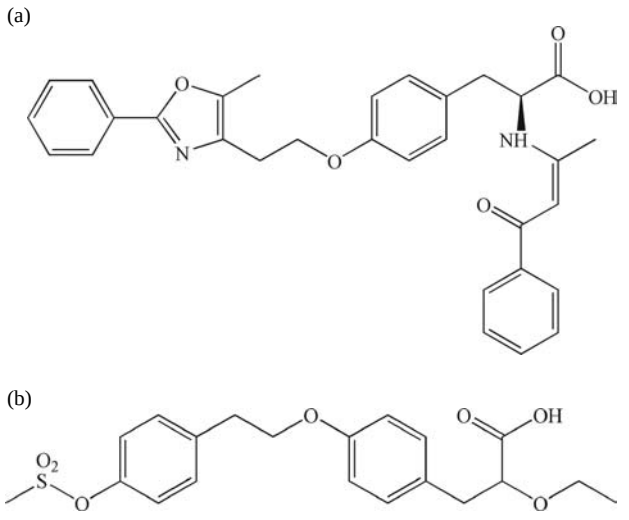

Figure 1. Chemical structures of ligand molecules to PPARα: (a) GW409544 and (b) AZ242.

PPARα and various ligand molecules for proposing new medicines controlling the PPARα functions.

Because PPARα is a nuclear receptor, only the chemical substances passing through the nucleus membrane can be a ligand of PPARα. More than 200 kinds of chemicals were considered as the ligand [9], including the fatty acids with long chain, the fibrate anti-hyperlipaemia medicines and the phthalic esters used as a plastic plasticiser. In our previous study [10], we investigated stable structures and electronic properties for the complexes of mouse PPARα and phthalate, as well as adipate esters, by molecular simulations based on the classical molecular mechanics (MM) and molecular orbital (MO) methods.

In the present study, we obtain the solvated structures of the complexes with human, mouse and rat PPARα and GW by classical MM calculations considering solvating water molecules explicitly. In addition, the electronic properties of these structures are investigated by the *ab initio* fragment MO (FMO) method. Based on the FMO results, we attempt to elucidate how the specific interactions between the amino acids of PPARα and GW ligand are changed for human, mouse and rat PPARα. This information may be useful for predicting the toxicity of new chemicals to the human body based on the biomedical studies for the experimental animals such as mouse and rat.

2. Details of calculations

2.1 Construction of the PPARα+GW structure for human, mouse and rat

As with our previous study [10], the initial structures of the LBD for human, mouse and rat PPARα were constructed based on the X-ray crystal structure of the complex with human PPARα and GW (PDB ID: 1K7L) [8]. As for the crystal structure of human PPARα, the 1I7G [11] structure is also registered in PDB. However, there are some missing amino acids in the 1I7G structure. Therefore, we employed the 1K7L structure in the present study. The 1K7L structure contains a tetramer of the LBD of human PPARα. By using the molecular simulation program HyperChem [12], we extracted a monomer (chain A) from the tetramer to construct the initial structure of the human PPARα+GW complex.

To construct the structure of mouse PPARα, we examined the difference in the sequence of amino acids between human and mouse PPARα. The LBD of these PPARα contains 267 amino acids. Among them, 21 amino acids are different [7], as shown in Figure 2(a) and (b). We thus replaced these 21 amino acids in human PPARα by the amino acids corresponding to mouse PPARα and optimised the structures of the replaced amino acids by the classical MM calculation based on the AMBER force field [13]. In this optimisation, we replaced one amino acid and optimised its structure by fixing the other part, in order to prevent the side chains of the replaced amino acids from bending, and binding them to the main chain. This procedure was repeated sequentially for the 21 amino acids to obtain the initial structure of the mouse PPARα+GW complex. In addition, the initial structure of the rat PPARα+GW complex was constructed in the same way. As shown in Figure 2(a) and (c), there are 19 amino acid differences between human and rat PPARα [7], so that these amino acids were replaced and optimised by the classical MM calculation. In this way, as a first step of our study for the PPARα+GW complexes, we investigated local minimum structures around the experimentally obtained one for the human PPARα+GW complex (PDB ID: 1K7L) [8]. The long-time molecular dynamics simulations, considering solvent water molecules explicitly, are currently running, and based on the results, we attempt to obtain grovel minimum structures of the PPARα+GW complexes.

In molecular simulations for proteins, we assume the protonation of histidine amino acids, because X-ray crystal structure analysis is difficult to determine the position of hydrogen atom for histidine. In the present study, we employed the uncharged histidine, since PPARα has a large positive charge, if we assume the positively charged histidine. We considered two types of the binding position of hydrogen atom in the imidazole ring of histidine to construct the following two structures of PPARα: one has histidine (HID) in which a hydrogen atom binds the δ site of the imidazole ring, and the other has histidine (HIE) with a hydrogen atom at the ε site of the imidazole ring. For both structures, their total energies were compared to obtain a more stable structure having the HIE. Therefore, the results for the PPARα+GW complexes with HIE are shown hereafter.

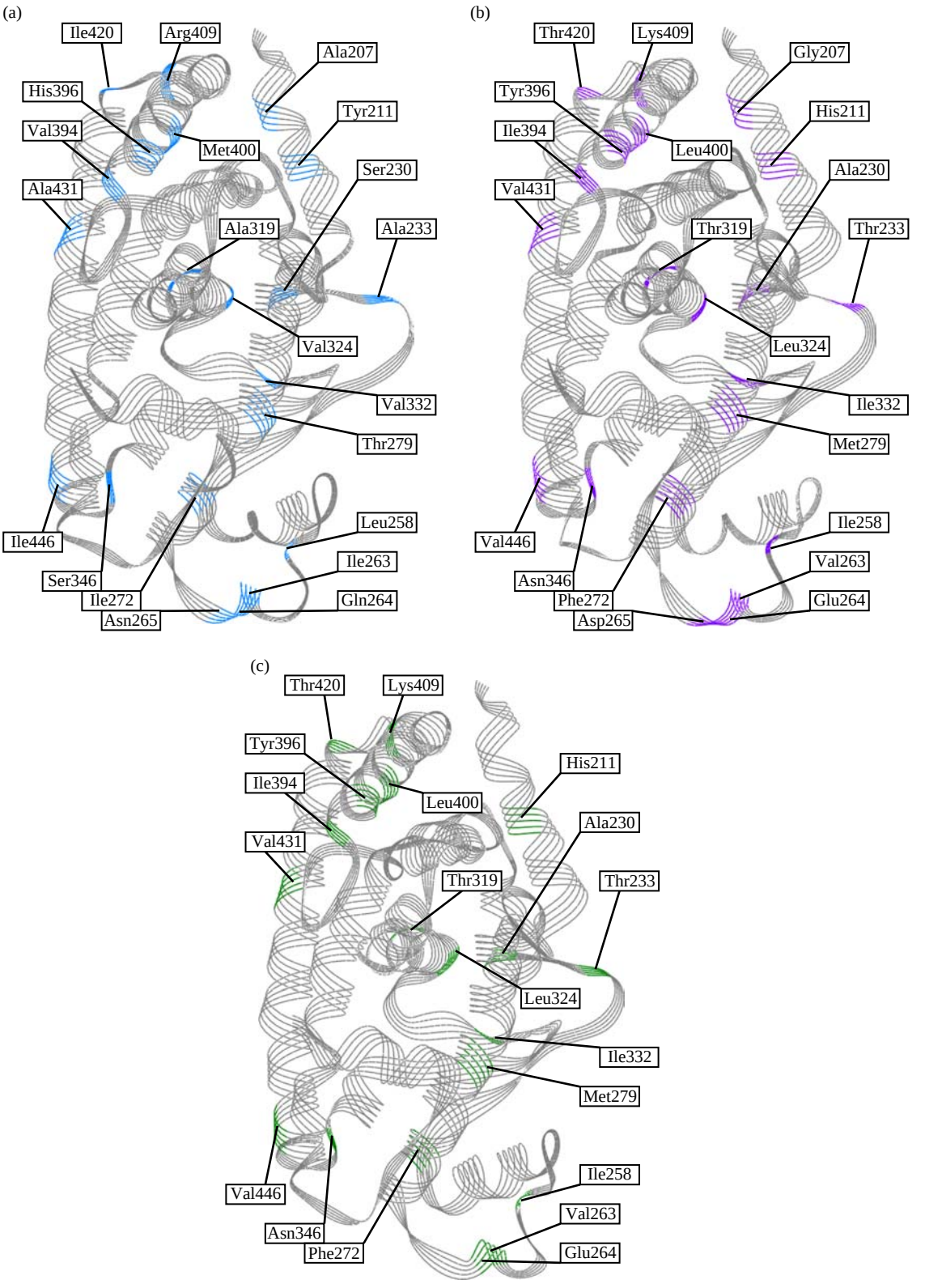

Figure 2. Difference in amino acids between (a) human, (b) mouse and (c) rat PPARα.

In the classical MM calculations, parameters in the force field are indispensable. The AMBER force field [13] has parameters for all amino acids of proteins. However, there is no parameter provided for the GW ligand. We thus performed the restrained electrostatic potential (RESP) calculation [14] for the structure of GW in the human PPARα+GW complex, because the GW structure is changed largely in the ligand-binding pocket of human PPARα from that in vacuum. In the RESP calculation, the MP2/6-31G(d,p) method was used to obtain the charge distribution of GW in high accuracy. Based on the results, atomic charges for each atom of GW were determined, and the electric charge parameters for the AMBER force field were produced. Furthermore, the AMBER parameters for van der Waals interactions, the bond length between atoms, torsion angles and dihedral angles were selected from the prepared AMBER parameters. The *ab initio* MO calculation program Gaussian 03 [15] was used for the RESP calculations.

By using the AMBER force field [13], the structures of the PPARα+GW complexes for human, mouse and rat were optimised in water. In our previous study [10], the effect of solvation was considered with the continuum solvent approximation. On the other hand, we here explicitly consider the solvating water molecules existing within 8 Å distance from the surface of the complex, in order to elucidate the contribution of water molecules to the specific interactions between PPARα and GW.

The MM calculation program AMBER9 [16] was used for these optimisations, in which the PARM99 [14] and TIP3P [17] force fields were used for the complex and water molecules, respectively. The threshold value of the energy gradient for the convergence of optimisation was set to be 0.0001 kcal/mol/Å.

2.2 Analysis of specific interactions between PPARα and GW

The electronic properties of these optimised structures in water were investigated by the FMO calculations to elucidate which amino acids in PPARα are important for the specific interactions between PPARα and GW. In FMO calculations, we used the FMO program ABINIT-MP version 4.1 [18,19]. The FMO method was developed by Kitaura et al. [20] as a technique to be able to calculate the electronic properties of huge molecules. The FMO calculation was employed in earlier studies regarding the nuclear receptors [21–24] as well as other proteins [25]. In this method, the target molecule is divided into the unit called fragment, and the electronic properties of the target molecule are estimated from the electronic properties of the monomers and dimers of the fragments. Since the electronic properties of the dimers are calculated in FMO, we can obtain the interaction energies between fragments.

It is not practical to calculate the electronic properties of the PPARα+GW complex including all the crystal and solvating water molecules by the *ab initio* FMO method. We thus considered only the water molecules existing within 5 Å distance from the surface of the complex. Each amino acid of PPARα and GW are assigned as a fragment, respectively. This fragmentation enables us to evaluate the interaction energy between the amino acid of PPARα and GW. To investigate the interaction between GW and the surrounding amino acids more accurately, we treated GW, the amino acids and water molecules existing within 5 Å distance from GW by the MP2/6-31G method, while the other amino acids and water molecules were treated by the HF/6-31G method. From the comparison of the obtained interaction energies, it was elucidated which amino acids of PPARα or water molecules are important for the specific interactions between PPARα and GW.

3. Results and discussion

3.1 Comparison of optimised and experimental structures for human PPARα+GW

To examine the adequacy of the present optimisation procedure based on the AMBER force field [13], we first compared the optimised structure of the human PPARα+GW complex with its X-ray crystal structure [8]. The root mean square distances (RMSDs) between the two structures are 1.34 Å for all atoms and 1.19 Å for only Cα atoms, indicating that the optimised structure of human PPARα+GW is comparable to the X-ray crystal structure. The two structures are superimposed in Figure 3. There is no remarkable difference between them in the ordered domains with the α-helix or β-sheet structure, while the flexible part in the loop structure between the domains has a different structure between the optimised and experimental ones.

In addition, to confirm how the optimised human PPARα structure around GW is comparable to that obtained by the X-ray analysis [8], these PPARα structures around GW are compared in detail. In the previous experiment [8], it was considered that 28 amino acids of human PPARα and one water molecule are important for the specific interactions between human PPARα and GW, as shown in Figure 4. We thus analysed the distances between GW and these amino acids or the water molecule for both the experimental and optimised structures. In the experimental structure, among the 28 amino acids shown in Figure 4, 25 amino acids, except for Ile317, Ile241 and Val444, exist within a 4 Å distance from GW. While 27 amino acids, except for Glu251, exist around the GW in the optimised structure. Therefore, it was confirmed that the optimised structure of human PPARα around the GW ligand is comparable to the experimental one.

Figure 3. Comparison of the X-ray experimental [8] (blue) and our optimised (pink) structures for the human PPARα and GW complex (colour online).

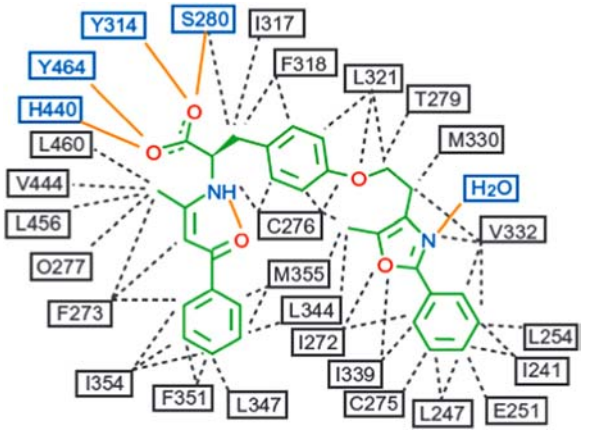

Figure 4. Amino acids of human PPARα interacting with GW in the experimentally obtained structure [8]. Hydrogen bonding and hydrophobic interactions between GW and PPARα or a bound water molecule are indicated by orange lines and broken lines, respectively (colour online).

3.2 Optimised structures of human, mouse and rat PPARα+GW complexes

In order to reveal the difference in the structure of PPARα+GW between human, mouse and rat, we compared their optimised structures. Among the 267 amino acids in the LBD of PPARα, 21 amino acids are different between human and mouse PPARα, while 19 amino acids are different between human and rat PPARα. We first investigated the RMSD between the LBDs of human, mouse and rat PPARα to elucidate the influence of the difference in amino acids on the structure of PPARα. Owing to the difference in amino acids, the RMSD for all atoms cannot be investigated between these PPARα. We thus analysed the RMSD for only Cα atoms to find that the RMSD values are 0.76 Å (human and mouse) and 0.79 Å (human and rat), respectively. Accordingly, the influence of the difference in amino acids on the whole structure of the LBD of PPARα was found to be small.

Furthermore, we investigated the structures around the GW ligand for mouse and rat PPARα. Table 1 lists the amino acids of PPARα existing near GW and the distances between these amino acids and GW. In the human and rat PPARα+GW complexes, GW has hydrogen bonds to Cys276, Ser280 and Tyr314, and these hydrogen bond distances are very similar for the human and rat PPARα+GW complexes; in the mouse PPARα+GW complex, three amino acids (Ser280, Tyr314 and His440) are hydrogen bonded to GW. It was thus elucidated that the hydrogen bonding structures between amino acids of PPARα and GW are remarkably different between human/rat PPARα and mouse PPARα.

In Figure 5, the structures of the human, mouse and rat PPARα+GW complexes are superimposed to elucidate the difference between them. The GW structures in these complexes are also superimposed and enlarged in the right-hand side of Figure 5. The structures of the ordered domains with α-helix or β-sheet in PPARα are similar to each other, while the structure of GW is remarkably different between the human and mouse/rat PPARα+GW complexes. As shown in Figure 5(a), the conformation of the right side chain of GW in the mouse PPARα+GW complex is changed by about 90° from that in the human PPARα+GW complex. Similarly, the conformation of GW in the rat PPARα+GW complex is different from that in the human PPARα+GW complex, as shown in Figure 5(b). The GW conformations in both mouse and rat PPARα are similar to each other (Figure 5(c)). These differences in GW structures are expected to cause the difference in specific interactions between GW and the amino acids of human, mouse and rat PPARα.

3.3 Specific interactions between human, mouse and rat PPARα and GW

To elucidate the difference in specific interactions between PPARα and GW for human, mouse and rat PPARα at the electronic level, we investigated the electronic properties of these PPARα+GW complexes by the *ab initio* FMO program [18,19]. Table 2 lists the total energies of the

Table 1. Amino acids existing near GW and the distances (Å) between these amino acids and GW for the human, mouse and rat PPARα+GW complexes.

Human PPARα		Mouse PPARα		Rat PPARα	
Amino acid	Distance	Amino acid	Distance	Amino acid	Distance
Cys276	2.11	Cys276	4.15	Cys276	2.02
Ser280	1.66	Ser280	1.63	Ser280	1.66
Tyr314	1.73	Tyr314	1.82	Tyr314	1.77
His440	4.41	His440	2.36	His440	3.86
Tyr464	2.56	Tyr464	2.60	Tyr464	2.53

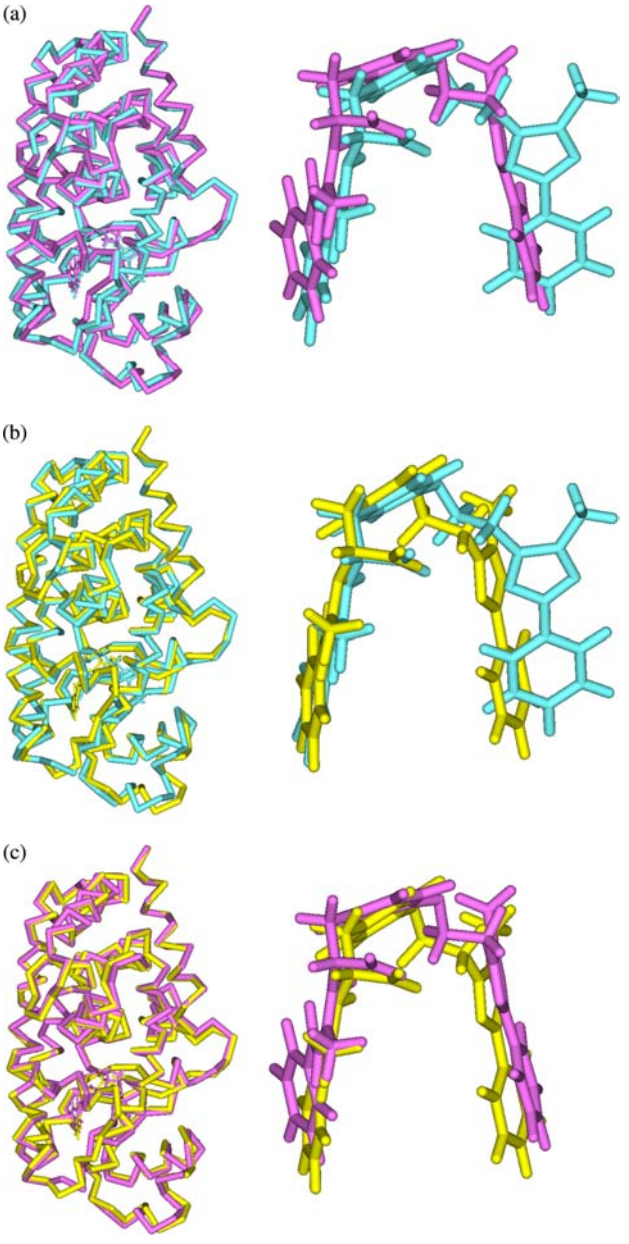

Figure 5. Comparison of the optimised structures for the PPARα+GW complexes: (a) human (blue) and mouse (pink), (b) human (blue) and rat (yellow) and (c) mouse (pink) and rat (yellow) (colour online).

complex, PPARα+water molecules and GW, and the estimated binding energies (BE) binding energy between PPARα+water molecules and GW. In the present study, the binding energy between PPARα+water molecules and GW was estimated as:

$$\mathrm{BE} = \mathrm{Total\,E(solvated\,PPAR\alpha + GW)} - \mathrm{total\,E(PPAR\alpha + water)} - \mathrm{total\,E(GW)}.$$

The binding energy for human PPARα+GW is the largest, indicating that the binding affinity of GW to human PPARα is larger than that for mouse and rat PPARα.

Furthermore, we investigated the interaction energies between each amino acid of PPARα and GW for human, mouse and rat PPARα. Table 3 lists the amino acids and their interaction energies with GW in a decreasing order of magnitude of attractive interactions. In all complexes, the positively charged Lys and Arg amino acids have large attractive interactions with GW, which has a negative charge. In particular, Lys358 has the largest attractive interaction in all complexes. As shown in Figure 4 and Table 1, these Lys and Arg amino acids do not exist around GW, however, they make a major contribution to the specific binding between PPARα and GW. This fact cannot be elucidated from the structure analysis of PPARα+GW alone. The present *ab initio* FMO calculations highlight that the electrostatic interactions between the positively charged amino acids (Lys and Arg) and the negatively charged GW are essential for the binding between PPARα and GW for human, mouse and rat.

In addition to these positively charged amino acids, uncharged Ser280 and Tyr314 amino acids have also large attractive interactions with GW for human and rat PPARα, while Ser280, Tyr314 and His440 have large attractive interactions for mouse PPARα. As shown in Figure 4, the experimental study [8] indicated that these amino acids are hydrogen bonded to the COO^- part of GW and considered to be important for the GW binding. The present FMO result (Table 3) for human PPARα+GW clarifies that Ser280 and Tyr314 have a rather large attractive interaction with GW. Therefore, it is expected that these

Table 2. Total energies (kcal/mol) of PPARα+GW+water complex, PPARα+water and GW, and the estimated binding energy (BE) between PPARα and GW.

	Total energies (Hartree)			
	PPARα+GW+Water	PPARα+Water	GW	BE (kcal/mol)
Human	−113799.5608	−112122.5216	−1676.8470	−120.58
Mouse	−114165.3950	−112488.4225	−1676.8305	−89.13
Rat	−114185.3196	−112508.3172	−1676.8426	−100.31

amino acids play an important role in the specific interactions between human PPARα and GW.

The interaction energies between all amino acids of PPARα and GW are shown in Figure 6, and their differences between human/mouse and human/rat are shown in Figure 7(a) and (b), respectively. In addition to the charged amino acids indicated by the thin blue lines in Figure 6, Ser280 and Tyr314 have large attractive interactions, while Tyr468 has a large repulsive interaction in all complexes. In addition, His440 of mouse PPARα and Cys276 of human and rat PPARα have large attractive interactions. The amino acids from 272 to 285 and from 314 to 333 have small contributions to the specific interactions between PPARα and GW.

As for the difference between human and mouse PPARα, Figure 7(a) elucidates that there are many amino acids (His440, Cys276, Asn265, Gln264, Gln277, Lys358, Val332, Leu460, Ser280, Cys275 and Phe273) having a remarkable difference (larger than 5 kcal/mol) in interaction energy; between human and rat PPARα, only three amino acids (Gln264, Gln277 and Ile272) have a large difference in interaction energy. Therefore, it can be concluded that the specific interactions between PPARα and GW are similar for human and rat, whereas they are remarkably different between human/rat and mouse PPARα. This result is consistent with the large difference (about 30 kcal/mol) in binding energy between human and mouse PPARα, as shown in Table 2.

To explain the reason for this difference in interaction energy, we investigated the structures of the amino acids of PPARα existing around GW. As shown in Figure 8, Ser280 and Tyr314 are strongly hydrogen bonded to the COO^- part of GW in all complexes; His440 and Cys276 exist on both sides of GW, so that the interactions between these amino acids and GW are largely dependent on the conformation of GW in the ligand binding pocket of PPARα. In the human (Figure 8(a)) and rat (Figure 8(c)) PPARα+GW complexes, the C═O part of GW exists near Cys276, so that the C═O part is hydrogen bonded to Cys276; in the mouse PPARα+GW complex (Figure 8(b)), the C═O part exists near His440. As a result, this part is hydrogen bonded to His440, not to Cys276. In this way, the specific interactions between the amino acids of PPARα and GW are dependent on the conformation and structure of GW. Figure 8 also elucidates that Thy464 is hydrogen bonded to the CH part of GW and not to the COO^- part of GW, resulting in the smaller interaction energy between Thy464 and GW, as shown in Figure 6 and Table 3.

Figure 9 illustrates the difference in the specific interactions between GW and the two α-helices of PPARα for human and mouse. As shown in Figure 9(a), the α-helix (4th α-helix composed of 268–292 amino acids) of human PPARα binds strongly to GW, resulting in the large interaction energies between these amino acids and GW, as shown in Figure 6(a), while GW has no hydrogen bond with His440. In contrast, in the mouse PPARα+GW complex (Figure 9(b)), the interaction between GW and the 4th α-helix is so weak that GW shifts to His440 and makes a hydrogen bond with His440. The rat PPARα+GW complex has a similar structure to the human one, shown in Figure 9(a). Consequently, the interaction between the 4th α-helix of PPARα and GW is considered to play an important role in distinguishing between human/rat PPARα and mouse PPARα.

Finally, in order to make clear the influence of the difference in amino acids on the specific interactions between GW and human, mouse and rat PPARα, we compared the interacting structures between GW and the 272nd and 332nd amino acids for human, mouse and rat PPARα. These amino acids are Ile and Val in human PPARα, while they are Phe and Ile in mouse and rat PPARα, as shown in Figure 10. The side chains of these amino acids exist near GW, so that it seems that they affect the structure of GW. In the human PPARα+GW complex, the two benzene rings existing at both ends of GW are oriented perpendicularly to each other, as shown in Figure 10(a); in the mouse and rat PPARα+GW complexes, the two benzene rings are stacked in parallel, because the side chain of Ile332 is longer than that of Val332 for human PPARα, and the GW chain existing near Ile332 rotates to make a parallel stacking shown in Figures 10(b) and (c). In mouse PPARα+GW (Figure 10(b)), the side chain of Phe272 is oriented perpendicularly to the two benzene rings of GW, so that the distance between the two benzene rings of GW is elongated; in rat PPARα+GW,

Table 3. Interaction energies (kcal/mol) between amino acids of human, mouse and rat PPARα and GW.

Human PPARα		Mouse PPARα		Rat PPARα	
Amino acid	Energy	Amino acid	Energy	Amino acid	Energy
Lys358	−45.38	Lys358	−39.21	Lys358	−47.57
Ser280	−33.86	Ser280	−28.41	Ser280	−33.70
Tyr314	−24.26	Lys448	−26.37	Lys448	−24.62
Lys448	−22.91	Tyr314	−24.96	Tyr314	−23.34
Arg465	−20.65	Arg465	−24.87	Arg465	−21.08
Lys310	−19.33	His440	−22.53	Lys266	−20.82
Lys257	−19.28	Lys310	−21.68	Lys310	−20.25
Lys266	−19.27	Lys449	−21.54	Lys449	−20.20
Arg388	−19.15	Arg388	−20.34	Arg348	−19.38
Arg348	−18.83	Lys292	−18.38	Arg388	−18.96
Lys449	−18.43	Arg348	−17.84	Lys292	−18.08
Arg341	−18.40	Lys257	−17.27	Arg341	−17.72
Lys364	−18.26	Lys266	−16.98	Lys364	−17.34
Lys345	−17.78	Arg341	−16.95	Lys257	−17.32
Arg271	−17.32	Lys364	−16.83	Lys345	−17.28
Lys292	−17.08	Lys349	−16.30	Lys349	−16.94
Cys276	−17.02	Arg226	−15.97	Arg226	−16.37
Lys349	−16.84	Lys224	−15.94	Lys224	−16.08
Lys224	−16.66	Lys216	−15.70	Arg271	−16.06
Arg226	−16.63	Arg434	−15.23	Lys222	−15.70
Lys222	−15.67	Lys345	−15.17	Lys216	−15.61
Lys216	−15.34	Lys429	−15.05	Lys429	−15.41
Lys429	−14.91	Arg271	−15.04	Arg434	−15.37
Lys252	−14.66	Lys222	−14.93	Lys252	−14.21
Arg434	−14.30	Lys252	−13.08	Lys327	−12.78
Lys327	−13.39	Lys327	−12.33	Cys276	−12.23
Lys232	−12.72	Arg209	−12.13	Arg209	−11.97
Arg209	−11.73	Lys232	−11.91	Lys232	−11.57
Lys425	−10.88	Lys425	−10.87	Lys425	−10.91
Arg409	−10.84	Lys399	−10.67	Lys399	−10.34
Gln277	−10.47	Lys409	−10.29	Lys409	−10.32
Lys399	−9.89	Leu460	−9.99	Lys208	−9.79
Lys208	−9.83	Lys208	−9.98	Lys204	−9.26
Lys204	−9.26	Lys204	−9.29	His440	−8.62
His440	−7.78	Ile332	−8.53	Met279	−7.18
Thr279	−7.14	Tyr464	−6.96	Val281	−6.73
Ile354	−5.06	Met279	−6.60	Ile332	−6.47
Val281	−4.82	Leu321	−4.71	Phe272	−6.42
Ala333	−4.81	Val281	−4.34	Leu321	−6.17
Leu321	−4.76	Thr285	−4.03	Leu460	−5.26
Thr285	−4.20	Thr283	−3.96	Ile354	−5.03
Leu460	−4.16	Gln445	−3.55	Tyr464	−4.84
Cys278	−3.97	Ile354	−3.45	Thr283	−4.42
Cys275	−3.73	Gln461	−3.42	Thr285	−4.41
Tyr464	−3.66	Thr319	−3.41	Cys278	−3.91
Thr283	−3.50	Cys278	−3.18	Met330	−3.56
Val284	−2.98	Met330	−2.95	Ile339	−3.28
Val332	−2.64	Ile317	−2.70	Thr319	−3.22
Phe318	−2.39	Val284	−2.67	Val284	−3.16
Met320	−2.31	Cys276	−2.57	Ser322	−2.92

Note: The amino acids are listed in the decreasing order of magnitude of attractive interaction.

the benzene rings of Phe272 and GW are stacked in parallel to each other, resulting in the packed structure of GW shown in Figure 10(c). As a result, the interaction energy between Phe272 of rat PPARα and GW is larger than that between Ile272 of human PPARα and GW, as shown in Figure 7(b).

Owing to the interaction between Phe272 of rat PPARα and GW, GW keeps the binding to the 4th α-

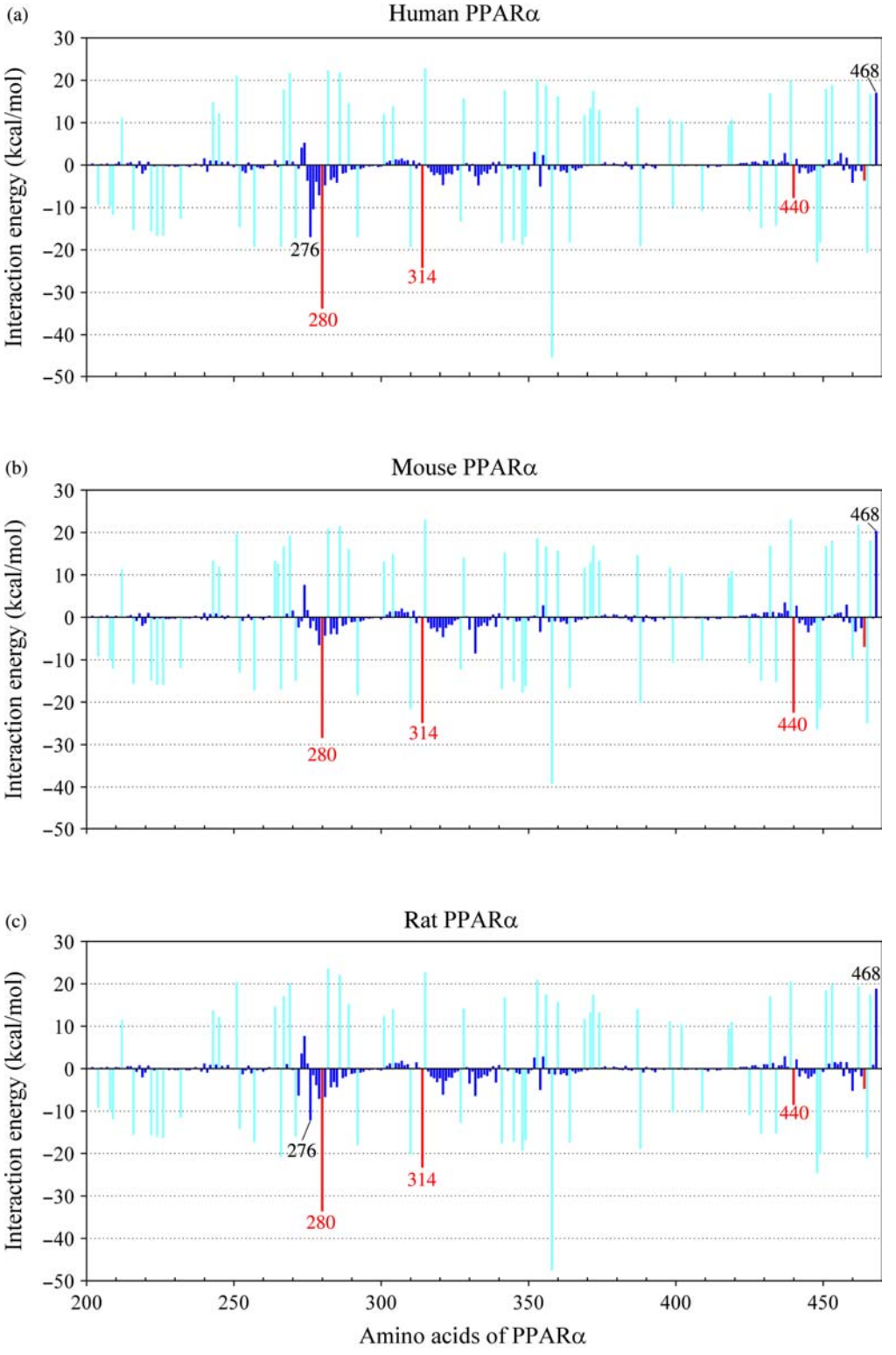

Figure 6. Interaction energies between GW and the amino acids of PPARα: (a) human, (b) mouse and (c) rat PPARα. Thin blue, red and dark blue lines represent the charged amino acids, the amino acids bonded to the COO^- part of GW and the other amino acids of PPARα, respectively (colour online).

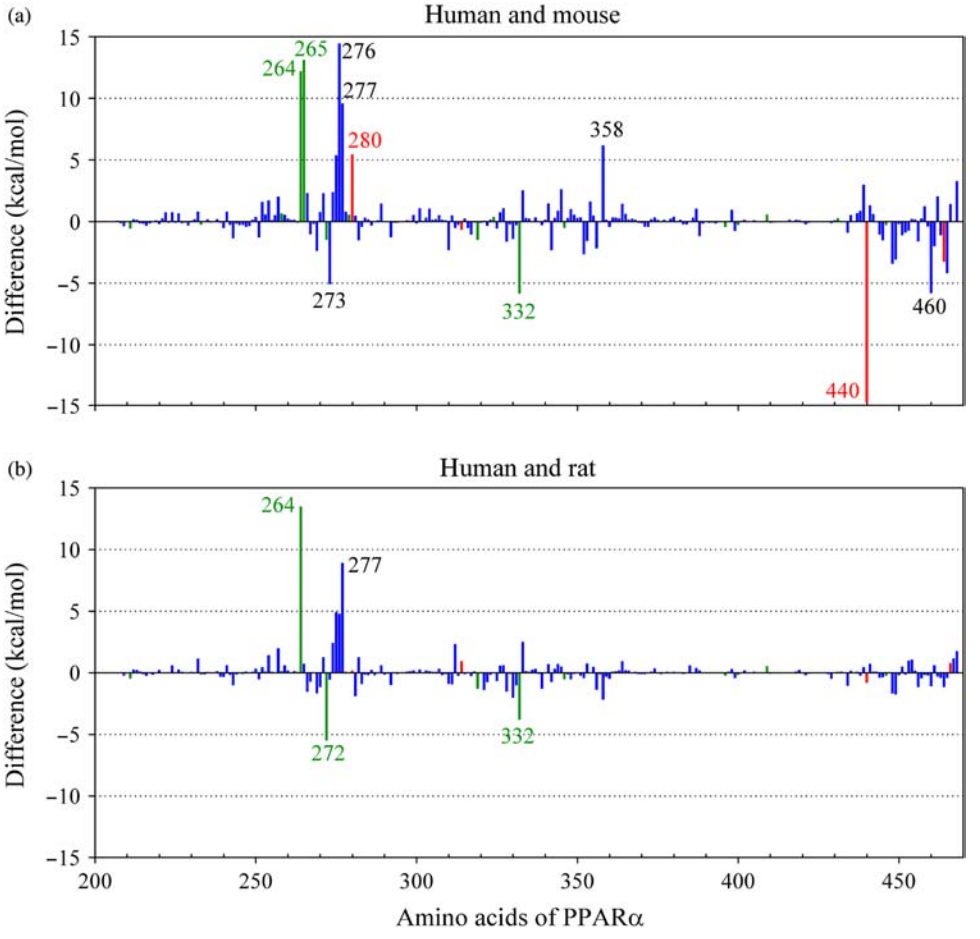

Figure 7. Difference in interaction energies between GW and the amino acids of PPARα: (a) between human and mouse and (b) between human and rat. Red, green and dark blue lines represent the amino acids bonded to the COO^- part of GW, the amino acids with different types between human and mouse/rat and the other amino acids of PPARα, respectively (colour online).

helix composed of 268–292 amino acids, as shown in Figure 9(a). In contrast, the weak interaction between Phe272 and GW in mouse PPARα+GW causes the shift of GW to His440, as indicated in Figure 9(b). Consequently, the present results elucidate that the difference in the 272th and 332th amino acids of the ligand binding site of PPARα affects largely the structure of GW as well as its interactions with PPARα, resulting in the large difference in the binding energy between GW and human, mouse and rat PPARα, as shown in Table 2.

3.4 Influence of amino acid mutation on interactions between human PPARα and GW

The difference in the interaction energies between GW and each amino acid of PPARα for human, mouse and rat is shown in Figure 7, where the green lines are for the amino acids with different types between human and mouse/rat PPARα. Among these amino acids, the 264, 265, 272 and 332 amino acids have a large difference in interaction energy with GW between human and mouse/rat PPARα. In particular, the interaction energy between GW and the 264 amino acid depends largely on the type of living organisms, indicating a possibility that this amino acid may cause the difference in binding affinity of GW for human, mouse and rat PPARα. In order to elucidate the influence of the 264 amino acid on the GW binding affinity, the 264 and/or 265 amino acids of human PPARα were mutated, and the stable structures and electronic properties were investigated in the same way as for the wild-type human PPARα+GW complex.

In human PPARα, the 264 and 265 amino acids are Gln264 and Asn265, while they are Glu264 and Asp265 (mouse PPARα), Glu264 and Asn265 (rat PPARα), respectively. The Glu and Asp amino acids are negatively charged, so that they have repulsive interactions with

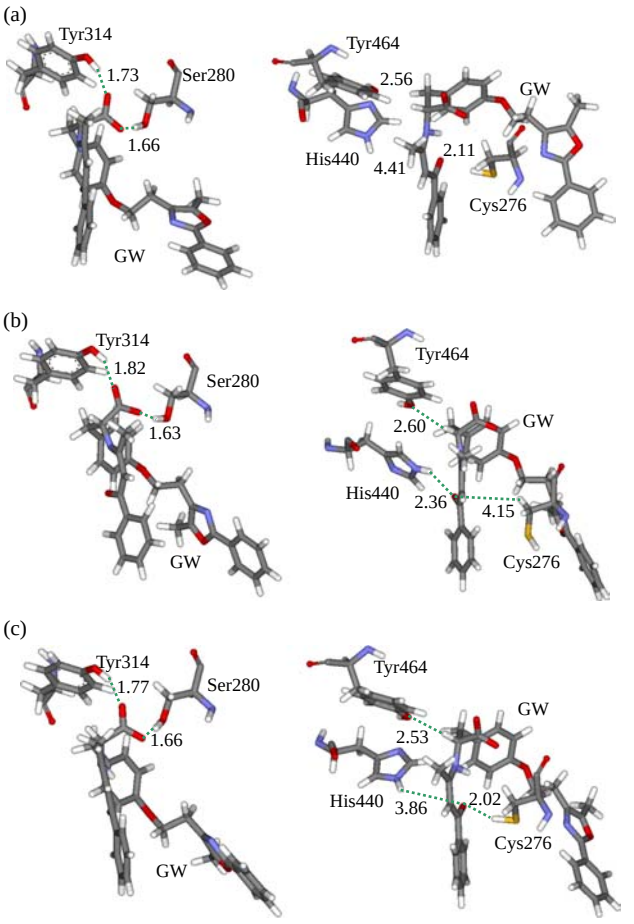

Figure 8. Structures and hydrogen bond distances (Å) between GW and amino acids of PPARα: (a) GW and human PPARα, (b) GW and mouse PPARα and (c) GW and rat PPARα.

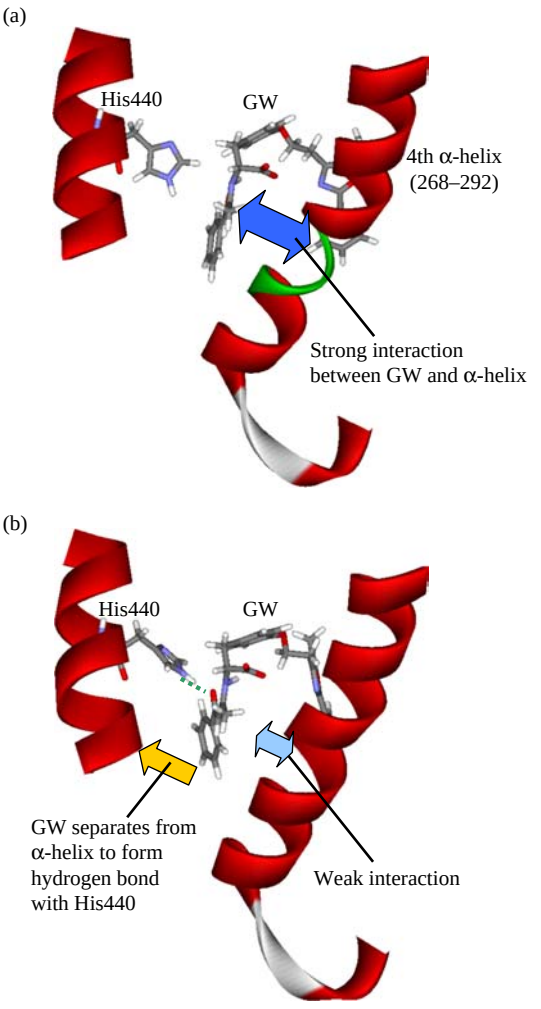

Figure 9. Interacting structures between GW and two α-helices and His440 of PPARα: (a) human and (b) mouse PPARα+GW.

the negatively charged GW. It can be considered that the binding energy between mouse PPARα and GW becomes much smaller than that for the human and rat PPARα+GW complexes, mainly because mouse PPARα has these negatively charged amino acids near GW. In order to investigate this effect in detail, we replaced Gln264 of human PPARα by Glu, and optimised the structure of the mutated human PPARα+GW complex to obtain the binding energy between the mutated PPARα and GW. In addition, by the mutation of Asn265 with Asp, the effect of the mutation of both the 264 and 265 amino acids was investigated.

As indicated in Table 4, the binding energy between human PPARα and GW is about 20 kcal/mol reduced by the mutation of the Gln264 to Glu264 amino acid.

Table 4. Total energies (kcal/mol) of PPARα+GW+water complex, PPARα+water and GW, and the estimated binding energy (BE) between human PPARα and GW.

	Total energies (Hartree)			
	PPARα+GW+Water	PPARα+Water	GW	BE (kcal/mol)
Wild type PPARα	−113799.5608	−112122.5216	−1676.8470	−120.58
264 Mutated PPARα	−113819.4574	−112142.4561	−1676.8451	−98.02
264, 265 Mutated PPARα	−113839.6137	−112162.6218	−1676.8386	−96.15

Notes: The results for the wild-type human PPARα and the mutated PPARα with the Gln264 → Glu mutation as well as the Gln264 and Asn265 → Glu and Asp mutations are compared.

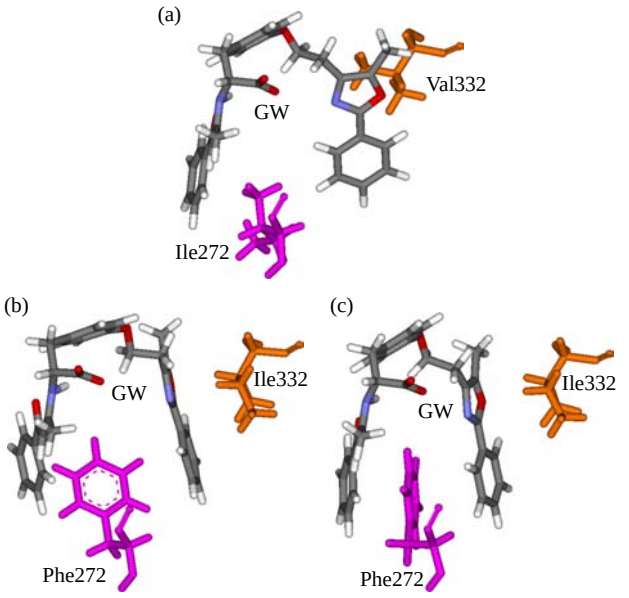

Figure 10. Interacting structures between GW and the 272nd and 332nd amino acids of PPARα: (a) human, (b) mouse and (c) rat PPARα.

On the other hand, the additional mutation of Asn265 to Asp265 amino acid does not largely affect the binding energy. Therefore, it is expected that the Gln264 amino acid of human PPARα is essential for the large binding energy between human PPARα and GW.

4. Conclusions

In the present study, we investigated the structures and electronic properties of the complexes with human, mouse and rat PPARα and GW ligand using the classical MM and *ab initio* FMO methods. The obtained results elucidate the interacting structures and specific interactions between these PPARα and GW at the electronic level. The positively charged amino acids (Lys and Arg) of PPARα were found to make a major contribution to the binding between PPARα and GW. In addition, it was highlighted that Ser280 and Tyr314 of human and rat PPARα have a large interaction energy with GW, while Ser280, Tyr314 and His440 of mouse PPARα have large energy.

Acknowledgements

This work was supported in part by grants from the Iketani Science and Technology Foundation, Tatematsu Foundation and CASIO Science Promotion Foundation.

References

[1] S. Mandard, M. Muller, and S. Kersten, *Peroxisome proliferator-activated receptor α target genes*, Cell Mol. Life Sci. 61 (2004), pp. 393–416.

[2] C.H. Lee, P. Olson, and R.M. Evans, *Lipid metabolism, metabolic diseases, and peroxisome proliferator-activated receptors*, Endocrinology 144 (2003), pp. 2201–2207.

[3] J.M. Peters, R.C. Cattley, and F.J. Gonzalez, *Role of PPAR alpha in the mechanism of action of the nongenotoxic carcinogen and peroxisome proliferator Wy-14,643*, Carcinogenesis 18 (1997), pp. 2029–2033.

[4] P.R. Devchand, H. Keller, J.M. Peters, M. Vazquez, and F.J. Gonzalez, *The PPARα-leukotriene B_4 pathway to inflammation control*, Nature 384 (1996), pp. 39–43.

[5] T. Kanayama, N. Kobayashi, S. Mamiya, T. Nakanishi, and J. Nishikawa, *Organotin compounds promote adipocyte differentiation as agonists of the peroxisome proliferator-activated receptor γ/retinoid X receptor pathway*, Mol. Pharmacol. 67 (2005), pp. 766–774.

[6] B.R. Henke, *Peroxisome proliferator-activated receptor alpha/gamma dual agonists for the treatment of type 2 diabetes*, J. Med. Chem. 47 (2004), pp. 4118–4127.

[7] D.F.V. Lewis, M.N. Jacobs, M. Dickins, and B.G. Lake, *Molecular modelling of the peroxisome proliferator-activated receptor α (PPARα) from human, rat and mouse, based on homology with the human PPARγ crystal structure*, Toxicol. In Vitro 16 (2002), pp. 275–280.

[8] H.E. Xu, M.H. Lambert, V.G. Montana, K.D. Plunket, L.B. Moore, J.L. Collins, J.A. Oplinger, S.A. Kliewer, R.T. Gampe, Jr, D.D. Mckee, J.T. Moore, and T.M. Willson, *Structural determinants of ligand binding selectivity between the peroxisome proliferator-activated receptors*, Proc. Natl. Acad. Sci. USA 24 (2001), pp. 13919–13924.

[9] S. Kersten and W. Wahli, *Peroxisome proliferator activated receptor agonists*, EXS 89 (2000), pp. 141–151.

[10] T. Nakagawa, N. Kurita, S. Kozakai, S. Iwabuchi, Y. Yamaguchi, M. Hayakawa, Y. Ito, T. Aoyama, and T. Nakajima, *Molecular mechanics and molecular orbital simulations on specific interactions between peroxisome proliferator-activated receptor PPAR-alpha and plasticizer*, J. Mol. Graph. Model. 27 (2008), pp. 45–58.

[11] P. Cronet, J.F. Petersen, R. Folmer, N. Blomberg, K. Sjoblom, U. Karlsson, E.L. Lindstedt, and K. Bamberg, *Structure of the PPARalpha and -gamma ligand binding domain in complex with AZ 242; ligand selectivity and agonist activation in the PPAR family*, Structure 9 (2001), pp. 699–706.

[12] *HyperChem 6.03*, Hyper Cube Inc., Florida, USA, 2000.

[13] P. Cieplak, W.D. Cornell, C. Bayly, and P.A. Kollman, *Application of the multimolecule and multiconformational RESP methodology to biopolymers: Charge derivation for DNA, RNA, and proteins*, J. Comp. Chem. 16 (1995), pp. 1357–1377.

[14] J. Wang, P. Cieplak, and P.A. Kollman, *How well does a restrained electrostatic potential (RESP) model perform in calculating conformational energies of organic and biological molecules?* J. Comp. Chem. 21 (2000), pp. 1049–1074.

[15] M.J. Frisch, G.W. Trucks, H.B. Schlegel, G.E. Scuseria, M.A. Robb, J.R. Cheeseman, J.A. Montgomery, Jr, T. Vreven, K.N. Kudin, J.C. Burant, J.M. Millam, S.S. Iyengar, J. Tomasi, V. Barone, B. Mennucci, M. Cossi, G. Scalmani, N. Rega, G.A. Petersson, H. Nakatsuji, M. Hada, M. Ehara, K. Toyota, R. Fukuda, J. Hasegawa, M. Ishida, T. Nakajima, Y. Honda, O. Kitao, H. Nakai, M. Klene, X. Li, J.E. Knox, H.P. Hratchian, J.B. Cross, C. Adamo, J. Jaramillo, R. Gomperts, R.E. Stratmann, O. Yazyev, A.J. Austin, R. Cammi, C. Pomelli, J.W. Ochterski, P.Y. Ayala, K. Morokuma, G.A. Voth, P. Salvador, J.J. Dannenberg, V.G. Zakrzewski, S. Dapprich, A.D. Daniels, M.C. Strain, O. Farkas, D.K. Malick, A.D. Rabuck, K. Raghavachari, J.B. Foresman, J.V. Ortiz, Q. Cui, A.G. Baboul, S. Clifford, J. Cioslowski, B.B. Stefanov, G. Liu, A. Liashenko, P. Piskorz, I. Komaromi, R.L. Martin, D.J. Fox, T. Keith, M.A. Al-Laham, C.Y. Peng, A. Nanayakkara, M. Challacombe, P.M.W. Gill, B. Johnson, W. Chen, M.W. Wong, C. Gonzalez, and J.A. Pople, *Gaussian 03 (Revision B.04)*, Gaussian, Inc., Pittsburgh, PA, 2003.

[16] D.A. Case, T.E. Cheatham, III, T. Darden, H. Gohlke, R. Luo, K.M. Merz, Jr, A. Onufriev, C. Simmerling, B. Qang, and R. Woods, *The Amber biomolecular simulation programs*, J. Comp. Chem. 26 (2005), pp. 1668–1688.

[17] W.L. Jorgensen, J. Chandrasekhar, J. Madura, R.W. Impey, and M.L. Klein, *Comparison of simple potential functions for simulating liquid water*, J. Chem. Phys. 79 (1983), pp. 926–935.

[18] T. Nakano, T. Kaminuma, T. Sato, K. Fukuzawa, Y. Akiyama, M. Uebayasi, and K. Kitaura, *Fragment molecular orbital method: Use of approximate electrostatic potential*, Chem. Phys. Lett. 351 (2002), pp. 475–480.

[19] T. Nakano, Y. Mochizuki, K. Fukuzawa, S. Amari, and S. Tanaka, *ABINIT-MP,* Ver. 4.1, 2007; software available at http://moldb.nihs.go.jp/abinitmp/.

[20] K. Kitaura, E. Ikeo, T. Asada, T. Nakano, and M. Uebayasi, *Fragment molecular orbital method: An approximate computational method for large molecules*, Chem. Phys. Lett. 313 (1999), pp. 701–706.

[21] K. Fukuzawa, K. Kitaura, M. Uebayasi, K. Nakata, T. Kaminuma, and T. Nakano, Ab initio *quantum mechanical study of the binding energies of human estrogen receptor with its ligands: An application of fragment molecular orbital method*, J. Comp. Chem. 26 (2005), pp. 1–10.

[22] T. Harada, K. Yamagishi, T. Nakano, K. Kitaura, and H. Tokiwa, Ab initio *fragment molecular orbital study of ligand binding to human progesterone receptor ligand-binding domain*, Naunyn Schmiedebergs Arch. Pharmacol. 377 (2008), pp. 607–615.

[23] M. Ito, K. Fukuzawa, T. Ishikawa, Y. Mochizuki, T. Nakano, and S. Tanaka, Ab initio *fragment molecular orbital study of molecular interactions in liganded retinoid X receptor: Specification of residues associated with ligand inducible information transmission*, J. Phys. Chem. B 112 (2008), pp. 12081–12094.

[24] K. Fukuzawa, Y. Mochizuki, S. Tanaka, K. Kitaura, and T. Nakano, *Molecular interactions between estrogen receptor and its ligand studied by the* ab initio *fragment molecular orbital method*, J. Phys. Chem. B 110 (2006), pp. 16102–16110.

[25] K. Dedachi, M.T.H. Khan, I. Sylte, and N. Kurita, *A combined simulation with* ab initio *MO and classical vibrational analysis on the specific interactions between thermolysin and dipeptide ligands*, Chem. Phys. Lett. 479 (2009), pp. 290–295.